Supplementary Table 1. Crystallographic data collection and refinement statistics (molecular replacement).

FH19-20/C3b TED/$GM1_g$	4ZH1.pdb
Data collection[a]	
Beamline	X06DA (SLS)
Wavelength (λ)	1.00
Space group	P1
Cell dimensions	
a, b, c (Å)	75.77, 82.57, 85.57
α, β, γ (°)	112.97, 111.43, 99.63
Resolution (Å)	50.0-2.24 (2.30-2.24)
R_{meas} (%)	6.1 (74.3)
I/σ(I)	15.63 (1.99)
Completeness (%)	97.6 (97.1)
Redundancy	3.5 (3.4)
Wilson B ($Å^2$)	54.9
Refinement	
Resolution (Å)	46.18-2.24
No. reflections	79286
Rwork / Rfree	18.09 / 22.84
No. Atoms	
Protein	9693
Ligand	158[b]
Water	448
B-factors ($Å^2$)	
Protein	66.9
Ligand	84.8[b]
Water	61.2
R. m. s. deviations	
Bond length (Å)	0.012
Bond angles (°)	1.39

[a] Values in parentheses are for highest-resolution shell. [b] $GM1_g$ and glycerol. B-factors for $GM1_g$ range from 76.3 $Å^2$ for chain E to 108.6 $Å^2$ for chain F which is loosely packed and not built to completeness due to insufficient density.

Supplementary Table 2. Crystal structures of proteins in complex with $GM1_g$ or larger glycans comprising $GM1_g$ with torsion angles for the GM1-like Neu5Acα2-3Gal linkage. Psi was approximated by subtracting 120° from the measured torsion (C2-O3-C3-C4). Only structures with correctly annotated mtz files in the protein data bank were used and densities were individually evaluated.

Protein	glycan	PDB code / chain	Phi [°] (C1-C2-O3-C3)	Psi [°] (C2-O3-C3-H3)	conformation
Human galectin-3 (Bian et al., 2011)	GM1	3AYC / B	190.3	-23.3	tC1
Human complement factor H	GM1	4ZH1 / D	300.5	-18.4	tC3
		4ZH1 / E	298.6	-16.6	tC3
		4ZH1 / F	309.0	-16.8	tC3
Agrocybe aegerita lectin (AAL) (Feng et al., 2010)	GM1	3M3Q / A	190.3	-26.4	tC1
Botulinum type A neurotoxin (Stenmark et al., 2008)	GT1b	2VU9 / A	301.6	-19.5	tC3
Botulinum type B neurotoxin (Berntsson et al., 2013)	GD1a	4KBB / A	178.6	3.1	tC1
		B	202.7	-34.3	tC1
Cholera toxin B pentamer (Merritt et al., 1997)	GM1	2CHB / D	189.0	-28.1	tC1
		E	188.2	-17.4	tC1
		F	190.0	-34.5	tC1
		G	184.4	-27.2	tC1
		H	188.2	-27	tC1
Cholera toxin B G33R mutant pentamer (Merritt et al., 1997)	GM1	1CT1 / F	173.8	-30.6	tC1
		G	175.3	-44.4	tC1
Cholera toxin B pentamer[a], (Merritt et al., 1998)	GM1	3CHB / E	191.6	-18.3	tC1

		H	183.1	-14.3	tC1
E.coli heat-labile entero-toxin B pentamer (Holmner et al., 2011)	GM1	2XRQ / D	160.0	32.4	tC1
		E	185.7	-10.2	tC1
		F	165.2	9.5	tC1
		G	170.2	10.3	tC1
		H	177.1	-1	tC1
E. coli EcxAB toxin (Ng et al., 2013)	GM1	4L6T / B	188.6	-20	tC1
		C	194.6	-20.3	tC1
		D	192.4	-21.2	tC1
		E	189.1	-19.2	tC1
		F	189.7	-21.2	tC1
Simian Virus 40 VP1 pentamer (Neu et al., 2008)	GM1	3BWR / A	187.0	-21.9	tC1
		C	182.6	-20.4	tC1
		E	180.9	-18.7	tC1
JC Mad-1 Polyomavirus (Ströh et al., 2015)	GM1	4X14 / B	189.7	-22.3	tC1
		C	190.4	-16	tC1
		D	198.5	-27.7	tC1
JC Polyomavirus geno-type 3 (Ströh et al., 2015)	GM1	4X0Z / B	189.9	-19.7	tC1
		C	187.2	-16.2	tC1
		D	195.9	-21.8	tC1
Adenovirus 37 fiber knob (Nilsson et al., 2011)	GD1a	3N0I / B	298.9	-14.8	tC3

[a] Only chains with sufficient density to support modeling of the Neu5Acα2-3Gal disaccharide are listed.

Supplementary Table 3. Crystal structures of proteins in complex with $GM3_g$ with torsion angles of the Neu5Acα2-3Gal linkage. Psi was approximated by subtracting 120° from the measured torsion (C2-O3-C3-C4). Only structures with correctly annotated mtz files in the protein data bank were used and densities were individually evaluated.

Protein	glycan	PDB code / chain	Phi [°] (C1-C2-O3-C3)	Psi [°] (C2-O3-C3-H3)	conformation
Human galectin-8 (Yoshida et al., 2012)	GM3	3VKM / A	296.1	9.0	tC3
		3VKM / B	293.1	9.5	tC3
Human galectin-3 CRD K176L mutant (Collins et al., 2014b)	GM3	4LBL / A	312.0	5.3	tC3
Human Siglec-5 (CD170) (Zhuravleva et al., 2008)	GM3	2ZG3 / A	299.1	-18.1	tC3
Complement factor H (Blaum et al., 2014)	GM3	4ONT / D	286.8	-12.1	tC3
		4ONT / E	291.2	-16.6	tC3
		4ONT / F	308.4	-19.2-	tC3
Murine sialoadhesin (May et al., 1998)	GM3	1QFO / A	290.1	-18.0	tC3
		1QFO / B	290.5	-22.1	tC3
Maackia amurensis leukoagglutinin (Imberty et al., 2000)	GM3	1DBN / A	289.5	2.1	tC3
		1DBN / B	289.7	2.1	tC3
Superantigen-like protein from *Staphylococcus aureus*[c]	3'SLN	4RGT / A	290.1	-19.1	tC3
		4RGT / B	288.7	-18.3	tC3
Endo-glycoceramidase II from *Rhodococcus sp.* (Caines et al., 2007)	GM3	2OSX / A	292.3	-1.2	tC3

Vibrio cholerae sialidase (Connaris et al., 2009)	GM3	2W68 / A	298.3	-23.1	tC3
		2W68 / B	279.1	-26.2	tC3
		2W68 / C	297.0	-30.0	tC3
Botulinum type C neuro-toxin (Yamashita et al., 2012)	GM3	4EN6 / B	187.2	-38.5	tC1
Botulinum type A neuro-toxin (Lee et al., 2013)	GM3	4LO5 / B	278.2	-21.3	tC3
Murine Polyomavirus (Stehle et al., 1994)	GM3	1SID / A	321.0	1.3	tC3
		1SID / B	298.8	12.6	tC3
		1SID / C	302.5	15.1	tC3
		1SID / D	320.4	-2.6	tC3
		1SID / E	310.2	6.1	tC3
		1SID / F	322.6	-6.5	tC3
Monkey B-lymphotropic polyomavirus VP1[a] (Neu et al., 2013)	3'SLN	4MBY / A	300.9	-28.0	tC3
Human polyomavirus V9 VP1[b] (Khan et al., 2014)	3SLN	4POS / A	297.0	-21.4	tC3
		4POS / B	297.9	-20.0	tC3
		4POS / D	295.8	-20.0	tC3
		4POS / E	295.9	-23.9	tC3
		4POS / F	297.8	-22.0	tC3
		4POS / G	295.9	-23.2	tC3
		4POS / H	300.6	-23.2	tC3
		4POS / I	299.1	-24.5	tC3
		4POS / J	292.4	-19.4	tC3
Adenovirus 37 fibre knob	GM3	1UXA / A	297.3	-11.5	tC3

(Burmeister et al., 2004)					
	GM3	1UXA / B	305.8	-10.4	tC3
T3D reovirus sigma1 (Reiter et al., 2011)	GM3	3S6X / A	180.2	-22.0	tC1
		3S6X / B	175.4	-12.8	tC1
		3S6X / C	300.0	-28.3	tC1
T1L reovirus sigma1 (Reiss et al., 2012)	GM3	4GU4 / A	187.2	-38.5	tC1
		4GU4 / B	192.8	-20.6	tC1
		4GU4 / C	192.7	-19.7	tC1
CRW-8 rotavirus VP8* (Yu et al., 2011)	GM3	3SIT / A	208.3	-18.0	tC1
		3SIT / B	298.5	-14.0	tC1
Avian influenza virus H1 haemagglutinin (Lin et al., 2009)	GM3	3HTT / A	187.0	-34.3	tC1
Avian influenza virus H7 haemagglutinin[a] (2003) (Yang et al., 2010)	3'SLN	3M5H / A	205.8	-58.9	tC1
		3M5H / E	155.3	0.7	tC1
Avian-origin influenza virus H1 haemagglutinin (2009) (Xu et al., 2012)	3'SLN	3UBQ / C	183.5	-5.5	tC1
		3UBQ / I	174.0	-13.7	tC1
		3UBQ / K	185.6	-12.8	tC1
Avian-origin human influenza virus H7 hemagglutinin (2013) (Shi et al., 2013)	3'SLNLN	4KOM / A	282.3	-3.8	tC3
Human influenza virus mutant H5 hemagglutinin (Xiong et al., 2013)	3'SLN	4CQW / A	187.3	-14.5	tC1

		4CQW / C	190.8	-20.9	tC1
		4CQW / E	199.3	-26.4	tC1
Canine influenza virus H3 haemagglutinin (2004) (Collins et al., 2014a)	3'SLN	4UO5 / A	156.2	21.4	tC1
		4UO5 / C	171.5	8.5	tC1
		4UO5 / E	168.0	7.8	tC1
Equine influenza virus H3 haemagglutinin (2004)[a] (Collins et al., 2014a)		4UO1 / A	136.9	30.8	tC1
		4UO1 / C	159.1	3.0	tC1
Seal influenza virus H3 haemagglutinin (2011) (Yang et al., 2015a)	3'SLN	4WA2 / A	197.4	-38.8	tC1
		4WA2 / B	190.4	-24.9	tC1
		4WA2 / C	181.7	-21.0	tC1
		4WA2 / E	188.6	-23.3	tC1
Seal influenza virus H3 hemagglutinin A/Taiwan/1/2013 (Yang et al., 2015b)	3'SLN	4WSU / A	229.4	-105.9	neither tC1 nor tC3[d]
Avian-origin human influenza virus H6 haemagglutinin (2013) (Tzarum N 2015)	3'SLN	4XKE / A	299.4	-12.9	tC3
Avian-origin influenza virus mutant H5 haemagglutinin (Xiong et al. 2015)	3'SLNS	5AJM / A	297.7	-20.1	tC3

[a] Only chains with sufficient density to support modeling of the Neu5Acα2-3Gal disaccharide are listed.

[b] There is a complex with GM3 in the database (4POR.pdb) which was omitted because the sugar binding is almost identical between the GM3 and 3'SLN complexes.

[c] To be published.

[d] Gal ring appears incorrectly placed.

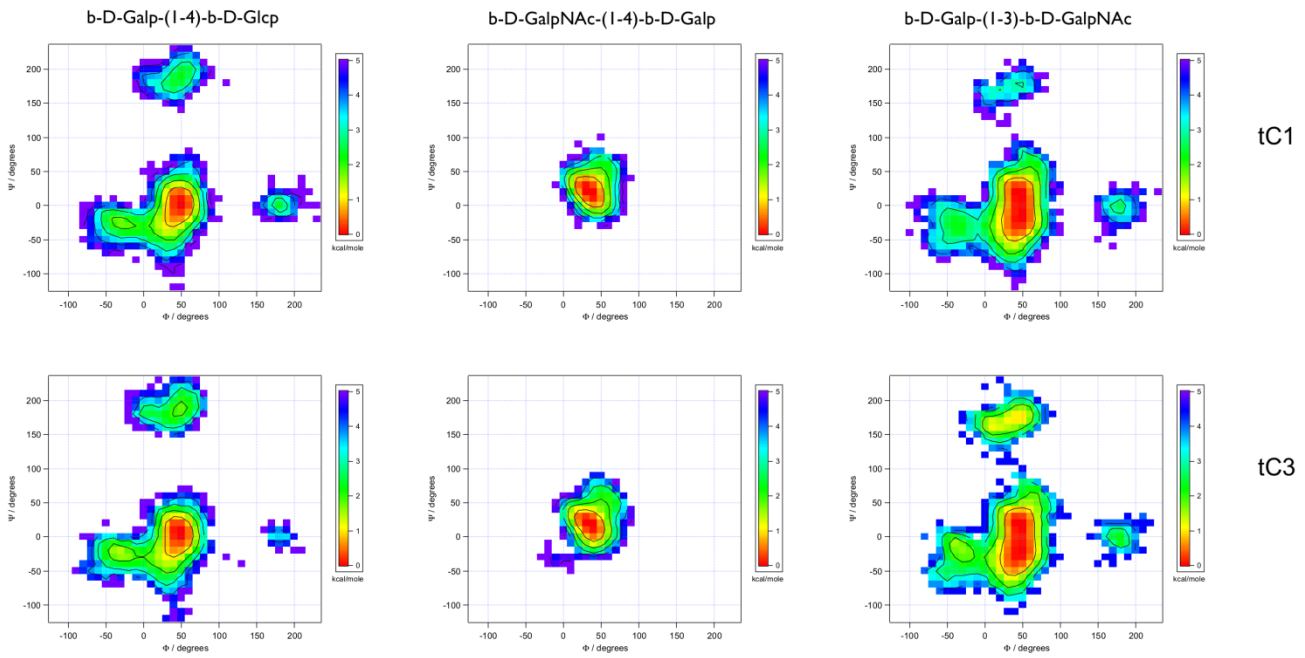

Supplementary Figure 1. Conformational Gibbs free energy φ/ψ Maps for free $GM1_g$ calculated separately for frames belonging to tC1 (φ = 190º, φ = -30º) and tC3 (φ = -65º, φ = 0º) minima of the Neu5Acα2-3Gal glycosidic linkage (φ = C1-C2-O3-C3, φ = C2-O3-C3-H3). The tolerance for assigning the frames was 30º. Definition of the torsions used for calculation of the maps: φ = H1-C1-Ox-Cx, φ = C1-Ox-Cx-Hx (x = linkage position).

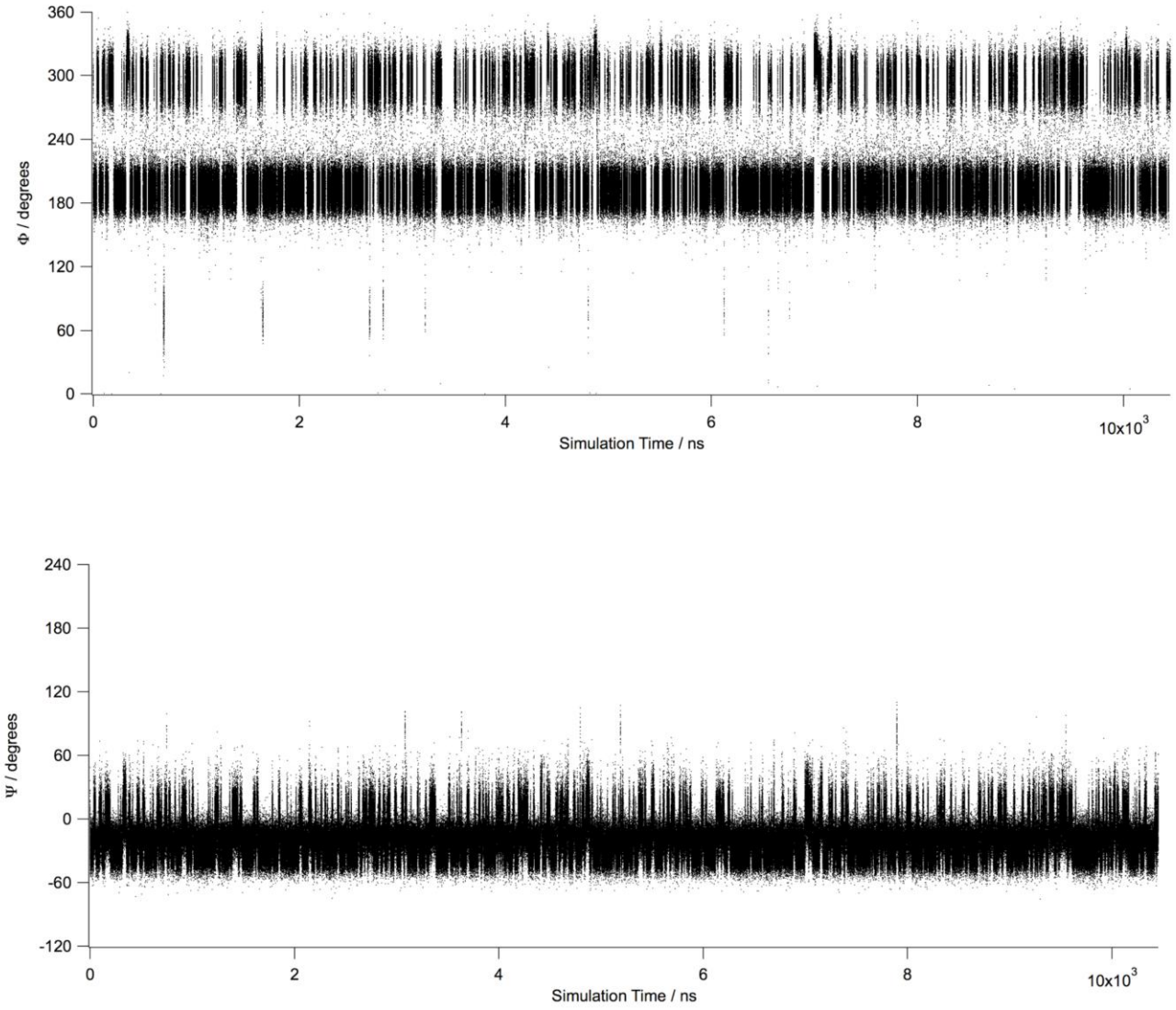

Supplementary Figure 2. Trajectories of phi and psi angles during simulation of the Neu5Acα2-3Gal glycosidic linkage in $GM1_g$.

References

Berntsson, R.P.-A., Peng, L., Dong, M., and Stenmark, P. (2013). Structure of dual receptor binding to botulinum neurotoxin B. Nat. Commun. *4*, 2058.

Bian, C.-F., Zhang, Y., Sun, H., Li, D.-F., and Wang, D.-C. (2011). Structural basis for distinct binding properties of the human galectins to Thomsen-Friedenreich antigen. PloS One *6*, e25007.

Blaum, B.S., Hannan, J.P., Herbert, A.P., Kavanagh, D., Uhrín, D., and Stehle, T. (2014). Structural basis for sialic acid–mediated self-recognition by complement factor H. Nat. Chem. Biol. *11*, 77-82..

Burmeister, W.P., Guilligay, D., Cusack, S., Wadell, G., and Arnberg, N. (2004). Crystal structure of species D adenovirus fiber knobs and their sialic acid binding sites. J. Virol. *78*, 7727–7736.

Caines, M.E.C., Vaughan, M.D., Tarling, C.A., Hancock, S.M., Warren, R.A.J., Withers, S.G., and Strynadka, N.C.J. (2007). Structural and mechanistic analyses of endo-glycoceramidase II, a membrane-associated family 5 glycosidase in the Apo and GM3 ganglioside-bound forms. J. Biol. Chem. *282*, 14300–14308.

Collins, P.J., Vachieri, S.G., Haire, L.F., Ogrodowicz, R.W., Martin, S.R., Walker, P.A., Xiong, X., Gamblin, S.J., and Skehel, J.J. (2014a). Recent evolution of equine influenza and the origin of canine influenza. Proc. Natl. Acad. Sci. U. S. A. *111*, 11175–11180.

Collins, P.M., Bum-Erdene, K., Yu, X., and Blanchard, H. (2014b). Galectin-3 interactions with glycosphingolipids. J. Mol. Biol. *426*, 1439–1451.

Connaris, H., Crocker, P.R., and Taylor, G.L. (2009). Enhancing the receptor affinity of the sialic acid-binding domain of Vibrio cholerae sialidase through multivalency. J. Biol. Chem. *284*, 7339–7351.

Feng, L., Sun, H., Zhang, Y., Li, D.-F., and Wang, D.-C. (2010). Structural insights into the recognition mechanism between an antitumor galectin AAL and the Thomsen-Friedenreich antigen. FASEB J. *24*, 3861–3868.

Holmner, Å., Mackenzie, A., Ökvist, M., Jansson, L., Lebens, M., Teneberg, S., and Krengel, U. (2011). Crystal Structures Exploring the Origins of the Broader Specificity of Escherichia coli Heat-Labile Enterotoxin Compared to Cholera Toxin. J. Mol. Biol. *406*, 387–402.

Imberty, A., Gautier, C., Lescar, J., Pérez, S., Wyns, L., and Loris, R. (2000). An unusual carbohydrate binding site revealed by the structures of two Maackia amurensis lectins complexed with sialic acid-containing oligosaccharides. J. Biol. Chem. *275*, 17541–17548.

Khan, Z.M., Liu, Y., Neu, U., Gilbert, M., Ehlers, B., Feizi, T., and Stehle, T. (2014). Crystallographic and glycan microarray analysis of human polyomavirus 9 VP1 identifies N-glycolyl neuraminic acid as a receptor candidate. J. Virol. *88*, 6100–6111.

Lee, K., Gu, S., Jin, L., Le, T.T.N., Cheng, L.W., Strotmeier, J., Kruel, A.M., Yao, G., Perry, K., Rummel, A., et al. (2013). Structure of a bimodular botulinum neurotoxin complex provides insights into its oral toxicity. PLoS Pathog. *9*, e1003690.

Lin, T., Wang, G., Li, A., Zhang, Q., Wu, C., Zhang, R., Cai, Q., Song, W., and Yuen, K.-Y. (2009). The hemagglutinin structure of an avian H1N1 influenza A virus. Virology *392*, 73–81.

May, A.P., Robinson, R.C., Vinson, M., Crocker, P.R., and Jones, E.Y. (1998). Crystal structure of the N-terminal domain of sialoadhesin in complex with 3' sialyllactose at 1.85 A resolution. Mol. Cell *1*, 719–728.

Merritt, E.A., Sarfaty, S., Jobling, M.G., Chang, T., Holmes, R.K., Hirst, T.R., and Hol, W.G. (1997). Structural studies of receptor binding by cholera toxin mutants. Protein Sci. *6*, 1516–1528.

Merritt, E.A., Kuhn, P., Sarfaty, S., Erbe, J.L., Holmes, R.K., and Hol, W.G. (1998). The 1.25 A resolution refinement of the cholera toxin B-pentamer: evidence of peptide backbone strain at the receptor-binding site. J. Mol. Biol. *282*, 1043–1059.

Neu, U., Woellner, K., Gauglitz, G., and Stehle, T. (2008). Structural basis of GM1 ganglioside recognition by simian virus 40. Proc. Natl. Acad. Sci. U. S. A. *105*, 5219–5224.

Neu, U., Khan, Z.M., Schuch, B., Palma, A.S., Liu, Y., Pawlita, M., Feizi, T., and Stehle, T. (2013). Structures of B-lymphotropic polyomavirus VP1 in complex with oligosaccharide ligands. PLoS Pathog. *9*, e1003714.

Ng, N.M., Littler, D.R., Paton, A.W., Le Nours, J., Rossjohn, J., Paton, J.C., and Beddoe, T. (2013). EcxAB is a founding member of a new family of metalloprotease AB5 toxins with a hybrid cholera-like B subunit. Struct. 1993 *21*, 2003–2013.

Nilsson, E.C., Storm, R.J., Bauer, J., Johansson, S.M.C., Lookene, A., Ångström, J., Hedenström, M., Eriksson, T.L., Frängsmyr, L., Rinaldi, S., et al. (2011). The GD1a glycan is a cellular receptor for adenoviruses causing epidemic keratoconjunctivitis. Nat. Med. *17*, 105–109.

Reiss, K., Stencel, J.E., Liu, Y., Blaum, B.S., Reiter, D.M., Feizi, T., Dermody, T.S., and Stehle, T. (2012). The GM2 glycan serves as a functional coreceptor for serotype 1 reovirus. PLoS Pathog. *8*, e1003078.

Reiter, D.M., Frierson, J.M., Halvorson, E.E., Kobayashi, T., Dermody, T.S., and Stehle, T. (2011). Crystal structure of reovirus attachment protein σ1 in complex with sialylated oligosaccharides. PLoS Pathog. *7*, e1002166.

Shi, Y., Zhang, W., Wang, F., Qi, J., Wu, Y., Song, H., Gao, F., Bi, Y., Zhang, Y., Fan, Z., et al. (2013). Structures and receptor binding of hemagglutinins from human-infecting H7N9 influenza viruses. Science *342*, 243–247.

Stehle, T., Yan, Y., Benjamin, T.L., and Harrison, S.C. (1994). Structure of murine polyomavirus complexed with an oligosaccharide receptor fragment. Nature *369*, 160–163.

Stenmark, P., Dupuy, J., Imamura, A., Kiso, M., and Stevens, R.C. (2008). Crystal structure of botulinum neurotoxin type A in complex with the cell surface co-receptor GT1b-insight into the toxin-neuron interaction. PLoS Pathog. *4*, e1000129.

Ströh, L.J., Maginnis, M.S., Blaum, B.S., Nelson, C.D.S., Neu, U., Gee, G.V., O'Hara, B.A., Motamedi, N., DiMaio, D., Atwood, W.J., et al. (2015). The Greater Affinity of JC Polyomavirus Capsid for α2,6-Linked Lactoseries Tetrasaccharide c than for Other Sialylated Glycans Is a Major Determinant of Infectivity. J. Virol. *89*, 6364–6375.

Swaminathan, S., Furey, W., Pletcher, J., and Sax, M. (1995). Residues defining V beta specificity in staphylococcal enterotoxins. Nat. Struct. Biol. *2*, 680–686.

Xiong, X., Martin, S.R., Haire, L.F., Wharton, S.A., Daniels, R.S., Bennett, M.S., McCauley, J.W., Collins, P.J., Walker, P.A., Skehel, J.J., et al. (2013). Receptor binding by an H7N9 influenza virus from humans. Nature *499*, 496–499.

Xu, R., McBride, R., Nycholat, C.M., Paulson, J.C., and Wilson, I.A. (2012). Structural characterization of the hemagglutinin receptor specificity from the 2009 H1N1 influenza pandemic. J. Virol. *86*, 982–990.

Yamashita, S., Yoshida, H., Uchiyama, N., Nakakita, Y., Nakakita, S., Tonozuka, T., Oguma, K., Nishikawa, A., and Kamitori, S. (2012). Carbohydrate recognition mechanism of HA70 from Clostridium botulinum deduced from X-ray structures in complexes with sialylated oligosaccharides. FEBS Lett. *586*, 2404–2410.

Yang, H., Chen, L.-M., Carney, P.J., Donis, R.O., and Stevens, J. (2010). Structures of receptor complexes of a North American H7N2 influenza hemagglutinin with a loop deletion in the receptor binding site. PLoS Pathog. *6*, e1001081.

Yang, H., Nguyen, H.T., Carney, P.J., Guo, Z., Chang, J.C., Jones, J., Davis, C.T., Villanueva, J.M., Gubareva, L.V., and Stevens, J. (2015a). Structural and functional analysis of surface proteins from an A(H3N8) influenza virus isolated from New England harbor seals. J. Virol. *89*, 2801–2812.

Yang, H., Carney, P.J., Chang, J.C., Villanueva, J.M., and Stevens, J. (2015b). Structure and receptor binding preferences of recombinant hemagglutinins from avian and human H6 and H10 influenza A virus subtypes. J. Virol. *89*, 4612–4623.

Yoshida, H., Yamashita, S., Teraoka, M., Itoh, A., Nakakita, S., Nishi, N., and Kamitori, S. (2012). X-ray structure of a protease-resistant mutant form of human galectin-8 with two carbohydrate recognition domains. FEBS J. *279*, 3937–3951.

Yu, X., Coulson, B.S., Fleming, F.E., Dyason, J.C., von Itzstein, M., and Blanchard, H. (2011). Novel structural insights into rotavirus recognition of ganglioside glycan receptors. J. Mol. Biol. *413*, 929–939.

Zhuravleva, M.A., Trandem, K., and Sun, P.D. (2008). Structural Implications of Siglec-5-Mediated Sialoglycan Recognition. J. Mol. Biol. *375*, 437–447.